DOI: 10.1515/amm-2016-0180

M. CECOTKA*, K. DYBOWSKI*, L. KLIMEK*#, S. LIPA*, A. RYLSKI*, D. SANKOWSKI**, R. WOJCIECHOWSKI**, M. BĄKAŁA**

EXAMINATION OF WETTING BY LIQUID ZINC OF STEEL SHEETS FOLLOWING VARIOUS KINDS OF ABRASIVE BLASTING

Abrasive blasting is one of the methods of surface working before hot-dip zinc-coating. It allows not only to remove products of corrosion from the surface, but it also affects the quality of the zinc coating applied later, thereby affecting wettability of surface being zinc-coated. The surface working can be done with different types of abrasive material.

The paper presents an effect of the method of abrasive blasting on wetting the surface of steel sheets by liquid zinc. Steels sheets following blasting with Al_2O_3 of different granularity and shot peening were examined. The worst wetting was recorded for a sample following shot peening – the results are below those for the reference test conducted for a sample not previously subjected to any treatment. Samples following abrasive blasting have similar parameters, regardless of the size of grain used for the treatment.

*Keywords***:** abrasive blasting; dip zinc coating; surface preparation, wettability

1. Introduction

Hot-dip zinc coating is nowadays successfully applied in machine industry to protect different types of steel products, such as steel sheets and tapes, against corrosion. The method has been known for many years and it is being constantly improved and perfected; with it, it is possible to obtain a tight coat at low cost, which provides effective protection in various aggressive environments and which adheres well to the base surface [1-4]. The technology of dip zinc-coating consists in creating a coat on the surface of steel items by dipping them in zinc bath. The quality of thus produced coat depends on a number of factors, such as the chemical composition of the steel, the composition of the bath, the method of preparing the surface, method of application, etc. In regard to the composition of steel, the quality of a coat is most affected by the content of silicon and phosphorus. If the content of Si in steel is greater than 0.04% and the sum of Si+2.5P lies within the range from 0.09% to 0.2%, then the Sandelin effect occurs, which manifests itself by excessive coat depth, its cracking and exfoliation from the base surface [5-10]. Various baths are used in order to reduce the adverse phenomena [11]. And so, the following products appeared on the market: WEGAL – an alloy of zinc with Al, Sn, Ni and Mn [12]; Galveko [13,14] – and alloy of zinc with Ni, Sn, Bi; and Magnelis – a zinc bath with admixture of Al and Mg.

The effects of zinc-coating of steel items are greatly affected by the condition of the surface. Abrasive blasting is currently one of the most effective methods of cleaning a surface and removing any kinds of foreign elements, such as scale or rust [15-17]. This treatment consists in setting in motion loose grains of abrasive material and giving them the appropriate velocity. In effect, kinetic energy accumulated in the grain turns into the work of machining. Surface layer, frequently contaminated with products of corrosion or scale, is removed at a small depth of the surface under treatment. This process produces a surface which is clear of any contamination, which can also be a base for paint coats, metal coats and conversion coats [16-18]. Basically, the course and outcome of the process of abrasive blasting is affected by such parameters as: type of the base surface and its condition, type of the abrasive agent, angle at which the abrasive agent hits the surface, the velocity of the agent and the duration of treatment. The process results in formation of a new surface layer whose parameters are different than before the treatment [19]. The surface developed in this manner and plastic deformations that occur during abrasive blasting intensify the interactions on the solid-liquid boundary during the process of dip-coating [20]. It is assumed that the surface roughness should be as high as possible for the proper adherence of the protective coat. However, the coat depth grows with the surface roughness, which makes the process increasingly uneconomical.

The microstructure of the coat is the product of complex physical processes, such as diffusion and dissolving metals and liquid. There have been many studies conducted recently regarding initial phenomena during the processes of bath metal coating [21-23].

The course and outcome of the process of zinc-coating is also affected by the surface wettability. In the first stage of contact of a steel item with the zinc bath, the solid surface is

* LODZ UNIVERSITY OF TECHNOLOGY, INSTITUTE OF MATERIALS SCIENCE AND ENGINEERING, 1/15 STEFANOWSKIEGO STR., 90-924 LODZ, POLAND
** LODZ UNIVERSITY OF TECHNOLOGY, INSTITUTE OF APPLIED COMPUTER SCIENCE, 18/22 STEFANOWSKIEGO STR., 90-924 LODZ, POLAND
# Corresponding author: leszek.klimek@p.lodz.pl

wetted by liquid zinc [24]. After the process of liquid spreading, the state of equilibrium is established with a specific wetting angle Θ. The process of liquid spreading over the solid surface is accompanied by various chemical processes, such as dissolving of the base material in the liquid or formation of a new phase [25]. Depending on the wetting angle, three situations can be identified: full wetting, when the angle takes the values close to zero, partial wetting at the angle Θ within the range of $0 < \Theta < 90°$ and no wetting when angle Θ lies in the range of $90 < \Theta < 180°$. The smaller the Θ angle (better wettability) the easier it is to apply a protective coat and to ensure effective protection against corrosion. When there is no wetting ($\Theta > 90°$) a coat cannot be applied from a liquid metal bath.

Considering how important wettability of an item by liquid metal is in a coat formation, it seems reasonable to determine it for different methods of the surface preparation. Therefore, the aim of the study is to examine the effect of abrasive blasting on steel surface wetting by liquid zinc.

2. Methodology of the study

Wettability was examined on an integrated platform for high-temperature automatic measurement of wettability and surface tension of solders, designed and made at the Institute of Applied Computer Science of the Lodz University of Technology. It is an automatic test stand which enables comprehensive testing of dynamic properties of surface – surface tension and wettability of liquid solders in the temperature range of up to 1000°C, in different process atmospheres [26-28].

2.1. Measurement method

Distribution of forces that act on a vertical plate and the measurement system before and after partial dipping is shown in Figure 1. The capillary force is determined by measurement of the difference between the forces that act on the measuring system.

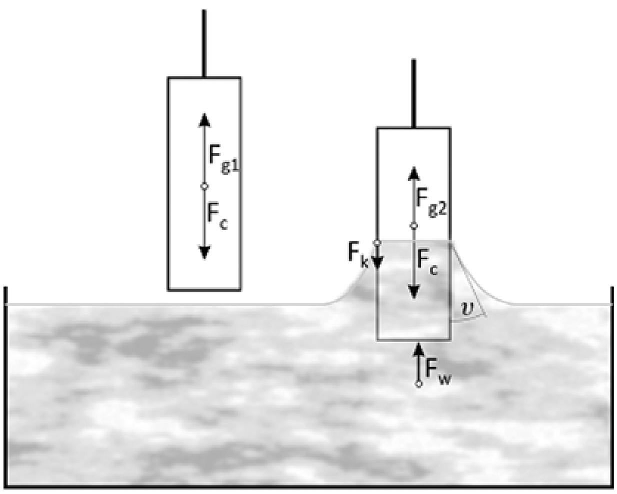

Fig. 1. Distribution of forces acting on a vertical plate

Before dipping:

- an upward force registered by the measuring system before dipping: F_{g1}
- the downward gravitation force: F_c

$$\sum_{i=1}^{i=n} F_{iy} = F_{g1} - F_c = 0 \qquad (1)$$

After dipping:

- an upward force registered by the measuring system after dipping: F_{g2}, while $F_{g2} > F_{g1}$
- Buoyancy, directed upwards: F_w
- Wetting capillary force: F_k

There are two possible models:

I – $0 \leq \theta \leq 90°$, then F_k is directed downwards,

II – $90° \leq \theta \leq 180°$, then F_k is directed upwards.

Model I was taken for further considerations, for which the sum of the projections of all the forces on the OY axis is:

$$\sum_{i=1}^{i=n} F_{iy} = F_{g2} + F_w - F_c - F_k = 0$$

In the steady state (θ is an equilibrium angle θ_0), for which the head surface of a sample is at the depth of z_b relative to the horizontal surface of the liquid plate, the force which acts on the measuring system is:

$$F_{g2} - F_{g1} = F_k - F_w$$

Further in the paper it is assumed that $F_{g2} - F_{g1} = F_M$

The buoyancy for the specific sample geometry and dipping depth is:

$$F_w = P_p \rho g z_b$$

Where: P_p – cross-section area of a sample, ρ – density of the liquid metal under study, g – gravitational acceleration, z_b – dipping depth.

The capillary force F_k is:

$$F_k = O_p \sigma_{LV} \cos\theta_0$$

Where: O_p – sample circumference, σ_{LV} – surface tension on the liquid-gas boundary, θ_0 – equilibrium wetting angle.

After transformations, the capillary wetting force F_k is determined by the following relationship:

$$F_k = \frac{F_M + P_p \rho g z_b}{O_p}$$

2.2. Dynamics of formation of the liquid meniscus

Of the fores considered in the previous paragraph, only the capillary force F_K is time-dependent, as the wetting angle when a solid is in contact with liquid changes from near 180° to the equilibrium value Θ_0.

The buoyancy changes in proportion in time from 0 to the maximum value which is a consequence of the depth to which the sample is dipped. However, in order to consider all the components independently, it must be assumed that the buoyancy reaches its equilibrium value before the capillary wetting force does. The diagram of the relationship between the wetting force and time in the plate dipping – withdrawing cycle is shown in Fig. 2 (the diagram is shown as an illustration only – the lengths of different sections, angles, etc. are taken arbitrarily).

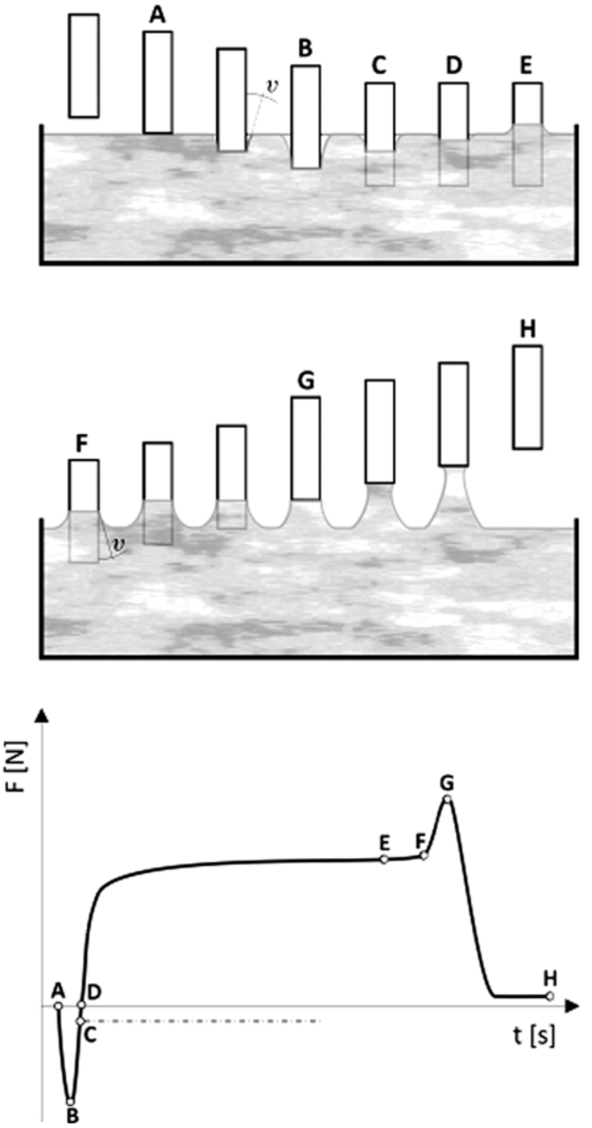

Fig. 2.The diagram of the relationship between the wetting force and time in the plate dipping – withdrawing cycle

At the beginning of the experiment, there is a contact of the sample head surface with the liquid. When a sample is further dipped the buoyancy acts along section A – C (which changes linearly with the dipping depth). At the same time, the liquid surface bends and a meniscus curved downwards is formed. The wetting angle ϑ increases until it reaches the minimum value (point *B*), close to 180°; at the same time, the sample is further dipped in liquid. This stage reflects the time of wetting incubation; bonds between atoms of both phases start to form and the phase boundary SL is formed. The stage of plate dipping ends at point C. Section C – E is wetting progression. Angle ϑ decreases until it reaches the equilibrium value ϑ_0 at point E. At this stage, the buoyancy is constant, the capillary force increases and it reaches zero at point D, where the wetting angle is 90°. From point D onwards, the wetting angle ϑ is an acute angle, until it reaches the limiting value at point E, when the stage of the plate removal starts. The stage of wetting the side surface of the plate ends at point G. The experiment ends at point H.

The diagram presented here is idealised, but it takes into account all the factors. In reality, the BC section can be very short, or it can even coincide with AB. If any inter-metallic phases are formed on the sample, then the DE section does not have to be horizontal. The EF section can be non-linear, because F_K can change as a result of the wetting hysteresis.

2.3. Methodology of the study

Samples with the dimensions of 0.8×8×40 mm, made of S355 MC steel for rolling were examined. The chemical composition of the steel is shown in Table 1.

TABLE 1

Chemical composition of the steel (%wt.)

Percentage content of elements										
C	Si	Mn	P	Cr	V	Cu	Al	Ni	S	Fe
0.09	0.013	0.8	0.012	0.015	0.07	0.03	0.035	0.015	0.015	remain-der

The samples were divided into five groups. The first group included the reference samples – with no surface treatment; the other four groups were subjected to abrasive blasting:

- shot peening with steel shots,
- blasting with aluminium oxide with the grain size of 50 μm (Rz = 11,9 μm)
- blasting with aluminium oxide with the grain size of 110 μm (Rz = 13,3 μm)
- blasting with aluminium oxide with the grain size of 250 μm (Rz = 16,4 μm)

The test of wetting with liquid zinc was performed on thus prepared samples. The purity of the zinc used for the experiment – 99.995%. The tests were conducted at the temperature of 430°C, in the reductive (95% argon and 5% hydrogen) and protective (nitrogen) atmosphere. The samples were heated above the plate of liquid zinc for 60 s and subsequently dipped to the depth of 5 mm for 120 s.

3. Results and discussion

The wettability for different options of abrasive blasting is shown in Figure 3.

The surface tension of Zn was determined on the basis of an empirical relationship provided by [29]. All the experiments were conducted at the temperature of 430°C. The surface tension at that temperature was determined to be 0.725 N/m.

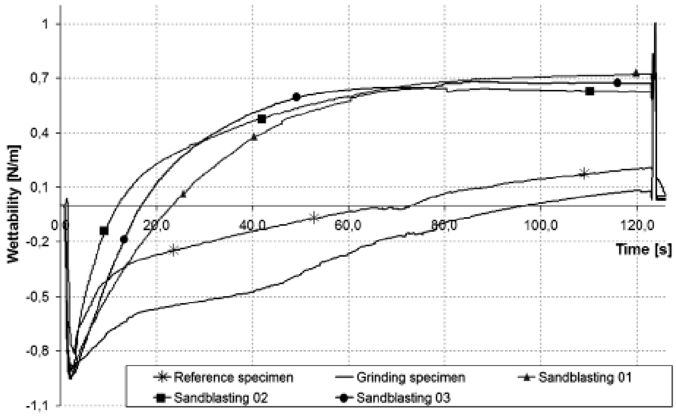

Fig. 3. Wettability of steel samples with differently prepared surface, registered during the process of dipping in liquid zinc at the temperature of 430°C

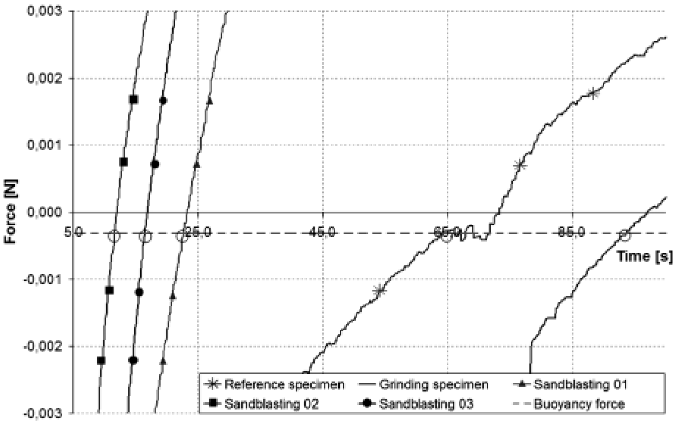

Fig. 5. A fragment of Fig. 3 which shows the changes of the wetting force and the buoyancy for the samples under study

This value provided the basis for plotting the characteristics of changes of the wetting angle against time for all the tested samples, which is shown in Figure 4.

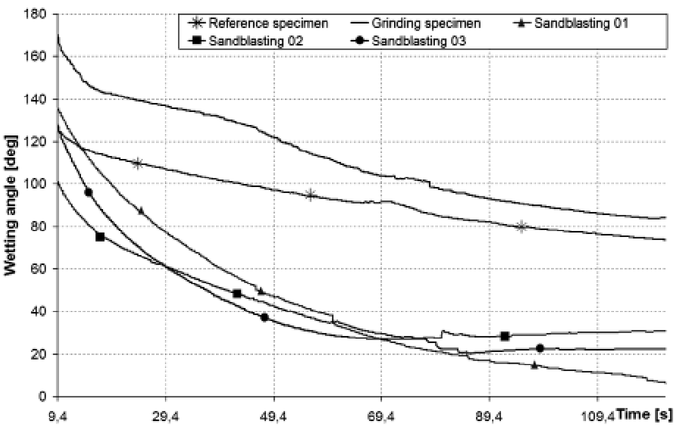

Fig. 4. Dynamics of changes of the wetting angle ϑ as a function of time for different variants of the sample surface preparation

Figure 4 shows that the best wettability is achieved for blasted samples for which the limiting wetting angle is close to 20°. On the other hand, the angle for the reference sample and one shot peened at the last stage of the wettability test was approx. 80°. This indicates poor wetting of the base surface.

Figure 5. Shows characteristic moments in time in which the wetting angle reaches $\vartheta = 90$. These points show the dynamics of the wetting process from the moment a sample is dipped $\vartheta = 90°$. In order to conduct an in-depth analysis of the dynamics of wetting the base surface, Fig. 5 shows fragments of the wetting forces and the buoyancy curves. The diagram indicates that the wetting process is much faster if a sample has been sandblasted. The time needed to achieve the wetting angle of $\vartheta = 90°$ is shown in Table 2

Figure 6 shows the changes of angle ϑ and the wetting force F_k [N/m] as a function of time for a sandblasted sample 03.

TABLE 2

The time needed to achieve the wetting angle of $\vartheta = 90°$ for different options of surface working

Surface working option	**Ref. sample**	**shot peening**	**Sandblasting 01**	**Sandblasting 02**	**Sandblasting 03**
Time [s]	64.6	94.0	22.9	12.0	16.8

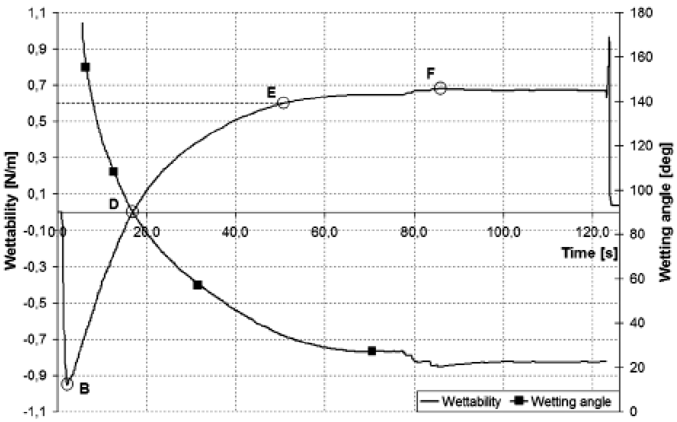

Fig. 6. The changes of angle ϑ and the wetting force F_k [N/m] and buoyancy as a function of time for a sandblasted sample 03

The diagram shows that during time t = 1.0 s, the head surface comes into contact with the molten solder bath. Initially, F_k decreases quickly and reaches the minimum (point B on the diagram) F_k = –0.95 N/m after time t = 2.3 s. The stage of dipping a sample to the depth of z_b = 5 mm ends after t = 2,7 s, for which F_k = –0.92 N/m. Time t_0 = 16.9 s (point D on the graph), is a moment in time for which the wetting angle $\vartheta = 90°$. The limiting value of the wetting force (point F on the graph) F_G = 0.68 N/m is reached after time t_C = 85.8 s. An additional parameter $t_{90\%}$ = 53.2 s (point E on the graph) reflects the required period of time until the wetting force reaches 90% of the limiting value of $F_{k90\%}$ = 0.612 N/m. The other parameters are listed in Table 3.

TABLE 3

Parameters of the dipping experiment for the samples

Parametr	Sample				
	Ref. sample	shot peening	Sandblasting 01	Sandblasting 02	Sandblasting 03
t_0 [s]	3	2	2	2	2
$t_{90\%}$ [s]	112	113	67	55	53
t_C [s]	122	121	122	80	86
F_G [N/m]	0,20	0,07	0.72	0.64	0.68
$t_{90\%}/t_C$[s]	0.92	0.93	0.55	0.69	0.61
$t_{90\%} - t_0$ [s]	119	111	65	53	51
$F_G/(t_{90\%} - t_0)$ [N/ms]	0.002	0.001	0.01	0.01	0.01

The parameters presented in Table 3 characterize the dynamics of wetting the base surface until the limiting value of F_G is reached.

4. Summary

A number of experiments have been conducted regarding the examination of wetting by liquid zinc of steel sheets following various kinds of abrasive blasting. Selected curves of wetting force and wetting angle are presented for samples following shot peening, sandblasting and for reference samples. The worst wetting was recorded for a sample following shot peening – the results are below those for the reference test conducted for a sample not previously subjected to any treatment. Much better wetting was observed for steel samples which have been sandblasted – the maximum wetting reaches 0.680 N/m, whereas it is 0.200 N/m for the reference sample and 0,140 N/m for a sample after shot peening. At the same time, wetting is accelerated in sandblasted samples, the wetting force remains constant from the 60th second onwards.

An integrated platform intended for an analysis of the dynamic properties of the surface is used to describe the wetting process quantitatively. The knowledge of these parameters helps to compare the results for different options of surface preparation and the process parameters. The results presented in the graphic form, registered in real time, allow for speedy analysis and process optimisation. The knowledge of the $t_{90\%}/t_C$ parameter helps to assess the dynamics of the wetting process.

Acknowledgements

This study was conducted within the project **GEKON1/05/213992/11/2014** project, co-financed by NCBiR and NFOŚiGW

REFERENCES

[1] H. Kania, P. Liberski, P. Podolski, Corrosion resistance of the zinc coatings obtained in modified zinc baths, Physico Chemical Mechanics of Materials **5**(2), 684-690 (2006).

[2] H. Kania, P. Liberski, P. Podolski, A. Gierek, J. Mendala, Corrosion resistance of zinc coatings obtained in high-temperature baths, Materials Science **39**(5), 652-657 (2003).

[3] F. C.Porter, Zinc Handbook, properties processing and use in design Marcel Dekker, New York (1991).

[4] A.R. Marder, The metallurgy of zinc-coated steel. Progress in Materials Science **45**, 191-271 (2000).

[5] J. Perlin, J. Hofman, V. Leroy, The influence of silicon and phosphorus on the commercial galvanization of mild steel, METALL **35**(9), 870-873 (1981).

[6] M. Yasuhiko, Effect of C and P addition on the corrosion of steel by molten zinc, Corros. Eng. **24**(4), 177-182 (1975).

[7] D. Kopyciński, E. Guzik, The kinetics of zinc coating growth on hyper-sandelin steels and ductile cast iron, Archives of Foundry Engineering **7**(4), 105-110 (2007).

[8] P. Liberski, Anticorrosion dip coating. WPŚ Gliwice (2013) (in Polish).

[9] M. Huckshold, Improving design guidance to avoid cracking of galvanized structural steelwork. Session: Steel and Galvanizing. Paper **3**, 1-6 Proceedings 22th International Galvanizing Conference. EGGA, Madrid (2009).

[10] H. Kania, P. Liberski, P. Podolski, A. Gierek, Some aspects of improvements in hot-dip galvanizing technology, Materials Engineering **2**, 775-782 (2004) (in Polish).

[11] V. Di Cocco, F. Iacoviello, S. Natali, Damaging micromechanisms in hot-dip galvanizing Zn based coatings, Theoretical and Applied Fracture Mechanics **70**, 91-98 (2014).

[12] J. Wesołowski, W. Głuchowski, Universal and saving zinc coating obtained in WEGAL bath, Conference papers, X Galvanizing Symposium, Ustroń (2003) 61-71 (in Polish).

[13] Ph. Beguin, M. Bosschaerts, D. Dhaussy, R. Pankert, M. Gilles, Galveco a solution for galvanizing reactive steel, Intergalva, Berlin (2000).

[14] R. Pankert, D. Dhaussy, Ph. Beguin, (Umicore Zinc Alloys & Chemicals) Mk. Gilles (Umicore Resaearch, Development Innovation) GALVECO – three years of presence on the market (2003).

[15] J. Andziak, The technology of preparing the steel surface for protective coating used in chemical industry, Anticorrosion Protection **7**, 172-175 (1983) (in Polish).

[16] J. Andziak, Theory and practice of abrasive blasting in preparing the base for protective coatings, Anticorrosion Protection **6,** 148-152 (1996) (in Polish).

[17] J. Andziak, The influence of the use of non-metallic abrasives on the quality of abrasive blast cleaned of metal base, Anticorrosion Protection **10**, 291-296 (1997) (in Polish).

[18] Z. Gawroński, A. Malasiński, J. Sawicki, Elimination of galvanic copper plating process used in hardening of conventionally carburized gear wheels, International Journal of Automotive Technology **11**(1), 127-131 (2010).

[19] W. Szymański, K. Pietnicki, L. Klimek, Assessing the surface of the prosthetic components after the abrasive blasting technology, Monograph. Biomaterials mechanics and scientific experiment in dentistry, edited by J. Kasperski, G. Chladek, PTIM, Zabrze 122-148 (2011) (in Polish).

[20] M. Płocińska, T. Płociński, J. Szawłowski, The morphology of zinc coating obtained on Armco iron with various plastic deformations, Materials Engineering **6**, 784-787 (2008) (in Polish).

[21] D. Kopyciński, The shaping of zinc coating on surface steels and ductile iron casting, Archives of Foundry Engineering **10**(1), 463-469 (2010).

[22] P. Liberski, A. Tatarek, B. Mendala, Investigation of the Initial Stage of Hot Dip Zinc Coatings on Iron Alloys with Various Silicon Contents, Solid State Phenomena **212**, 121-126 (2014).

[23] P. Liberski, A. Tatarek, B. Mendala, Investigation of the initial stage of hot dip zinc coatings on iron alloys with various silicon contents, Proc. of XXI Conference on Technologies and Properties of Modern Utility Materials (TPMUM 2013), Ed. TTP, Solid State Phenomena **212**, 121-126 (2014).

[24] A.M. Marder, The metallurgy of zinc-coated steel, Progress in Materials Science **45**, 191-271 (2000).

[25] W. Missol, The energy phase separation in metals, WŚK (1973) (in Polish).

[26] D. Sankowski, M. Bąkała, A. Albrecht, T. Koszmider, R. Wojciechowski, A. Rylski, Methodology for automatic measurement of dynamic surface properties – solderability and wettability, Materials Engineering **6**, 1064-1067 (2008).

[27] Z. Nitkiewicz, M. Bąkała, R. Wojciechowski, A. Albrecht, A. Rylski, The solderability of solder L-AG5P – the rating of selected parameters, Materials Engineering **6**, 1068-1071 (2008) (in Polish).

[28] M. Bąkała, R. Wojciechowski, D. Sankowski, A. Rylski, The wetting dynamics measurement system to research the properties and applications of modern materials, Microtherm 2015.

[29] W.L. Falke, A.E. Schwaneke, R.W. Nash, Surface Tension of Zinc: The Positive Temperature Cefficient, Metallurgical Transactions B. **8B**, 301-303 (1977).